Measurement of Cofactor Distances between $P_{700}^{\bullet+}$ and $A_1^{\bullet-}$ in Native and Quinone-Substituted Photosystem I Using Pulsed Electron Paramagnetic Resonance Spectroscopy†

Stephan G. Zech,‡ Arthur J. van der Est,§ and Robert Bittl*,‡

Max-Volmer-Institut für Biophysikalische Chemie und Biochemie, Technische Universität Berlin, Strasse des 17. Juni 135, 10623 Berlin, Germany, and Fachbereich Physik, Freie Universität Berlin, Arnimallee 14, 14195 Berlin, Germany

Received April 1, 1997; Revised Manuscript Received June 2, 1997⊗

ABSTRACT: The radical pair $P_{700}^{\bullet+}Q^{\bullet-}$ (P_{700} = primary electron donor, Q = quinone acceptor) in native photosystem I and in preparations in which the native acceptor (vitamin K_1) is replaced by different quinones is investigated by pulsed EPR spectroscopy. In a two-pulse experiment, the light-induced radical pair causes an out-of-phase electron spin echo, showing an envelope modulation. From the modulation frequency, the dipolar coupling, and therefore the distance between the two cofactors, can be derived. The observation of nearly identical distances of about 25.4 Å between $P_{700}^{\bullet+}$ and $Q^{\bullet-}$ in all preparations investigated here leads to the conclusion that the reconstituted quinones are bound to the native A_1 binding pocket. Since the orientation of the reconstituted naphthoquinone relative to the axis joining $P_{700}^{\bullet+}$ and $Q^{\bullet-}$ differs drastically from that of the native vitamin K_1, it cannot be bonded to the protein in the same way as the native acceptor. This implies that the function of A_1 as an electron acceptor does not depend on the orientation or hydrogen bonding of the quinone.

Photosystem I (PS I)[1] is a transmembrane protein−pigment complex found in cyanobacteria and higher plants that mediates the light-induced electron transfer (ET) from plastocyanin to ferredoxin. Light excitation of the primary electron donor, P_{700}, causes an electron to be transferred via a series of acceptors, i.e. a chlorophyll *a* (A_0), a phylloquinone (A_1), and three Fe_4-S_4 clusters (F_X and $F_{A/B}$), to finally reduce ferredoxin on the stromal side of the thylakoid membrane. The primary donor cation $P_{700}^{\bullet+}$ is reduced by plastocyanin from the lumenal side.

In contrast to some purple bacterial reaction centers (bRC), where the arragement of the cofactors involved in the ET is known from high-resolution X-ray analysis (Deisenhofer *et al*., 1985; Allen *et al*., 1987; Chang *et al.*, 1991; Ermler *et al.*, 1994; Arnoux *et al.*, 1995), the plant photosystems are less well-characterized. In PS I, the location and orientation of the phylloquinone molecule A_1 (vitamin K_1, VK_1) have not yet been determined in the present 4 Å resolution X-ray electron density map (Krauss *et al.*, 1996). Thus, information on the binding of A_1 to the protein using alternative approaches is important.

In all photosynthetic reaction centers, a sequence of radical pairs (RP) is formed as a consequence of the light-induced ET. The state $P_{700}^{\bullet+}A_1^{\bullet-}$ is the first RP accessible to time-resolved EPR techniques. It has a lifetime $t_{1/e}$ of ≈280 ns at room temperature which is limited by the forward ET to F_X (Lüneberg *et al.*, 1994; MoënneLoccoz *et al.*, 1994; van der Est *et al.*, 1994). At a temperature of 150 K, ET past $A_1^{\bullet-}$ is blocked in about 50% of the RCs (in the presence of 65% glycerol). In this fraction, the lifetime of $P_{700}^{\bullet+}A_1^{\bullet-}$ is approximately 200 μs (Schlodder *et al.*, 1995). For a discussion of further details of the ET and the arrangement of redox cofactors in PS I, see recent reviews (Witt *et al.*, 1996; Brettel *et al.*, 1997).

It has been shown in several studies that precise information on the relative orientation of the two cofactors forming the RP $P_{700}^{\bullet+}A_1^{\bullet-}$ can be obtained from the transient EPR spectra of the RP state as reviewed in Angerhofer and Bittl (1996). The recent study of the X-, K-, and W-band spectra of $P_{700}^{\bullet+}A_1^{\bullet-}$ in protonated PS I from *Synechococcus elongatus* yielded the principal values of the **g**-tensor of $A_1^{\bullet-}$ and its orientation relative to the axis joining $P_{700}^{\bullet+}$ and $A_1^{\bullet-}$, i.e. the axis of the dipolar coupling Z_D (van der Est *et al.*, 1997). The larger anisotropy of the **g**-tensor of $A_1^{\bullet-}$ was discussed in terms of a difference in the hydrogen bonding in the A_1 site compared to VK_1 in a frozen alcoholic solution or, alternatively, assigned to the influence of charged amino acid residues. In agreement with an earlier K-band study of deuterated PS I (Stehlik *et al.*, 1989), it was shown that in the native system the orientation of the g_{xx}-axis of the $A_1^{\bullet-}$ **g**-tensor is parallel to the dipolar axis Z_D to within a few degrees (van der Est *et al.*, 1997).

In other transient EPR studies, PS I preparations with artifical quinone acceptors have been used to study the quinone binding to its protein environment (Sieckmann *et al.*, 1991; van der Est *et al.*, 1995). A large difference in the transient EPR spectra measured at X-band (9 GHz) as

† This work has been supported by grants from Deutsche Forschungsgemeinschaft (SFB 312, TP A1/A4) and NaFöG Berlin (to S.G.Z.).

* Corresponding author. Fax: +49-30-314-21 122. E-mail: bittl@pair.chem.TU-Berlin.DE.

‡ Technische Universität Berlin.

§ Freie Universität Berlin.

⊗ Abstract published in *Advance ACS Abstracts,* August 1, 1997.

[1] Abbreviations: A_0, chlorophyll primary electron acceptor; A_1, phylloquinone secondary electron acceptor; bRC, bacterial reaction center; *D*, dipolar coupling constant; DQ-d_{12}, deuterated duroquinone; ENDOR, electron nuclear double resonance; EPR, electron paramagnetic resonance; ESE, electron spin echo; ESEEM, electron spin echo envelope modulation; ET, electron transfer; $F_{A/B}$ and F_X, iron−sulfur centers; *J*, isotropic exchange coupling; mw, microwave; NQ-d_6, deuterated 1,4-naphthoquinone; P_{700}, primary electron donor; PS I, photosystem I; Q, quinone acceptor; RP, radical pair; SFT, sine Fourier transform; τ_d, decay time constant; VK_1, vitamin K_1; Z_D, dipolar coupling axis.

S0006-2960(97)00754-X CCC: $14.00 © 1997 American Chemical Society

well as at K-band (24 GHz) has been found, if the native VK_1 is replaced by deuterated 1,4-naphthoquinone (NQ-d_6). This difference has been explained as a consequence of an altered orientation of the substituted NQ-d_6 compared to the native VK_1.

A valid criticism against the reliability in quinone substitution work after organic solvent extraction of A_1 is the additional extraction of some chlorophyll antenna molecules. Thus, quinone reconstitution could take place at a variety of vacant sites other than the A_1 site. Under these circumstances, altered quinone orientations should be expected which would not reflect the properties of the A_1 binding site in the protein. The transient EPR spectra yield the relative orientations of the **g**-tensors and the dipolar interaction axis but do not give the exact location of the quinone. Thus, although the forward ET to the reconstituted NQ-d_6 is intact and the recombination rate is on the same order of magnitude as in the native PS I (Sieckmann *et al.*, 1991), more conclusive evidence for substitution into the A_1 site is highly desirable.

One way of addressing this question is to determine the distance between the two cofactors P_{700} and A_1. If the substituted quinones are bound to the A_1 site, then the distance should be the same as in intact PS I. This distance can be calculated if the dipolar coupling *D* between the two electron spins within the RP is known. Accurate values of *D* cannot be obtained from the transient EPR spectra, because for distances greater than ~20 Å the dipolar coupling is smaller than the inhomogeneous line width and determines only the degree to which the absorptive and emissive contributions overlap. Thus, *D* enters the calculated spectra only as a scaling factor but causes no change in the polarization pattern.

In contrast, pulsed EPR experiments on the RP state allow the dipolar coupling between the two spins to be explored precisely. In a two-pulse experiment, the spin-polarized RP creates an out-of-phase electron spin echo (ESE), showing a deep envelope modulation (ESEEM). The modulation frequency is governed by the spin−spin interaction between the two electron spins within the RP (Salikhov *et al.*, 1992; Tang *et al.*, 1994). It has been shown that both spin−spin interactions, the isotropic coupling, *J*, and the dipolar coupling, *D*, can be deduced from the Fourier-transformed echo modulation (Dzuba *et al.*, 1995; Zech *et al.*, 1996; Bittl & Zech, 1997). For native PS I from *S. elongatus*, a distance of 25.4 ± 0.3 Å between $P_{700}^{\bullet+}$ and $A_1^{\bullet-}$ has been obtained by pulsed EPR spectroscopy which is about 3 Å shorter than the corresponding cofactor distance of 28.4 ± 0.3 Å measured in Zn-substituted bRCs (Zech *et al.*, 1996; Bittl & Zech, 1997). For PS I from spinach, the same distance of about 25 Å has also been determined recently (Dzuba *et al.*, 1997b).

To summarize, transient EPR spectra are very sensitive to the orientation of the two cofactors with respect to the dipolar coupling axis but not to the magnitude of the dipolar coupling. The modulation of the out-of-phase echo measured in a pulsed EPR experiment, on the other hand, shows a particular sensitivity to the dipolar and isotropic coupling constant but is almost insensitive to **g**-tensor arrangements and hyperfine couplings. The two spectroscopic methods are therefore complementary and should be used together to gain as much structural information on the RP state as possible.

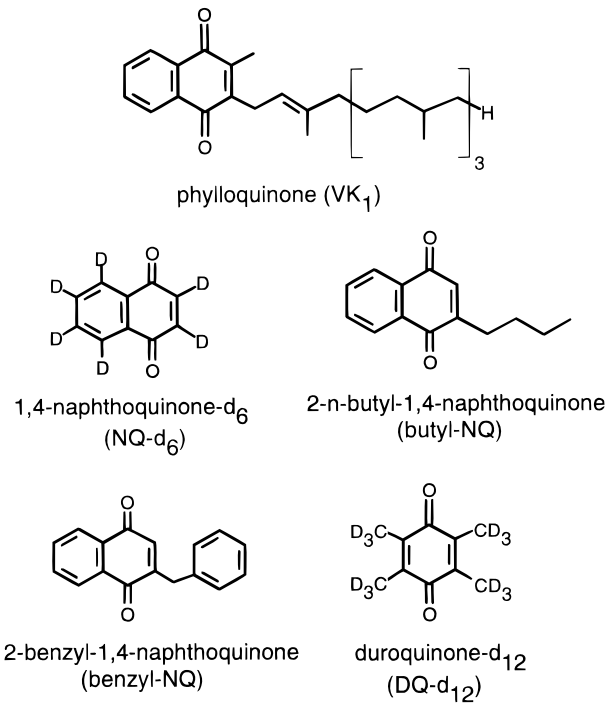

FIGURE 1: Structural formulas of phylloquinone (top) and the quinones used for A_1 reconstitution.

In this paper, we present pulsed EPR experiments on the RP state $P_{700}^{\bullet+}A_1^{\bullet-}$ in native PS I from *Synechocystis* PCC6803 as well as in preparations in which the acceptor quinone A_1 (VK_1) is substituted by either NQ-d_6, 2-benzyl-1,4-naphthoquinone (benzyl-NQ), 2-*n*-butyl-1,4-naphthoquinone (butyl-NQ), or perdeuterated duroquinone (DQ-d_{12}) (see Figure 1 for structural formulas). The out-of-phase echo modulation yields similar distances between $P_{700}^{\bullet+}$ and $Q^{\bullet-}$ in the native and the quinone-substituted samples and is a strong indication for binding of the substituted quinones at the A_1 site. The implications of altered quinone orientations within the A_1 binding pocket on the properties of this site are discussed in terms of differences in the hydrogen bonding situation between the artificial quinones and the native VK_1.

MATERIALS AND METHODS

Sample Preparation. Vitamin K_1 -depleted, lyophilized PS I particles from *Synechocystis* PCC6803 were prepared according to the method of Biggins and Mathis (1988) as described previously (Sieckmann *et al.*, 1991). The quinone-extracted particles were then rehydrated and incubated at 5 °C with a 1.0 mM solution of a given quinone. NQ-d_6 was provided by H. Zimmermann (MPI Heidelberg), and DQ-d_{12} was obtained from W. Lubitz (Technische Universität Berlin). Benzyl-NQ and butyl-NQ were a kind gift of W. Oettmeier (Ruhr Universität Bochum). The latter two quinones were purified by MPLC prior to use. Incorporation of the quinone into the reaction centers was monitored by comparing the relative amplitudes of the transient EPR spectra of the triplet state of P_{700} formed by recombination from $P_{700}^{\bullet+}A_0^{\bullet-}$ and the RP state $P_{700}^{\bullet+}Q^{\bullet-}$. After reconstitution of the quinone, the samples were stored in liquid nitrogen until further use.

EPR Experiments. All EPR measurements were performed at a temperature of 150 K using the experimental setup described previously (Bittl & Zech, 1997). The pulse

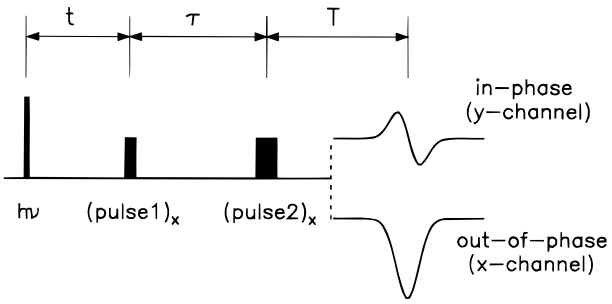

FIGURE 2: Pulse scheme used for the measurement of the coupling between the two electron spins. The laser pulse ($h\nu$) creates the radical pair $P_{700}^{\bullet+}Q^{\bullet-}$. After $t \approx 800$ ns, two mw pulses along the *x*-direction with a length of 8 and 16 ns and pulse spacing τ are applied. After the time $T \approx \tau$, the electron spin echo is detected in the out-of-phase channel (*x*-channel). At this time, the in-phase echo (*y*-channel) is almost zero. The modulation of the out-of-phase echo is monitored by recording the echo intensity at increasing values of τ and T.

sequence depicted in Figure 2 has been used: laser flash−t−(pulse 1)$_x$−τ−(pulse 2)$_x$−T−quadrature detection. The delay time t between the laser flash and the first mw pulse has been set to a constant value of $t \approx 800$ ns to prevent influences of the zero quantum coherence on the echo shape (Dzuba *et al.*, 1996a). The detection time T and the magnetic field B_0 were adjusted to the maximum of the out-of-phase echo intensity. The mw pulse lengths have been set to 8 ns for pulse 1 and 16 ns for pulse 2. The maximum out-of-phase echo intensity occurred at a mw power damped by about 1 dB from a nominal value of 1 kW. It should be noted that the modulation frequency of the out-of-phase echo is independent of the actual flip angle of the mw pulses (Bittl & Zech, 1997). An adjustment of the flip angles to 90 and 180°, respectively, as used for the derivation of the analytical expressions (Salikhov *et al.*, 1992), is therefore not necessary. The calibration of in-phase and out-of-phase signals has been performed as described in detail previously (Bittl & Zech, 1997). Monitoring the maximum of the echo intensity at increasing values for the evolution time τ and detection time T reveals the out-of-phase echo modulation pattern as shown in Figures 3 and 4. Up to 256 ESEEM traces (512 points with 8 ns increments of τ) were accumulated to increase the signal-to-noise ratio.

RESULTS

Qualitative Analysis. Shown in Figure 3 are the envelope modulations of the out-of-phase echo of the RP state $P_{700}^{\bullet+}A_1^{\bullet-}$ in protonated samples of native PS I and of $P_{700}^{\bullet+}Q^{\bullet-}$ in quinone-reconstituted preparations. The top curve in Figure 3 depicts the echo modulation for PS I from *Synechocystis* PCC6803 containing the native VK_1. This echo modulation is very similar to that described recently for PS I from *S. elongatus*. The damping of the echo modulation measured in the native sample corresponds to the one observed in a PS I sample from *S. elongatus* in aqueous buffer without addition of glycerol (Zech *et al.*, 1996). For a native sample of *S. elongatus* containing glycerol as a cryoprotectant a weaker damping of the ESEEM has been observed (Bittl & Zech, 1997).

The modulation frequency of the ESEEM which is determined by the dipolar and isotropic coupling parameters is identical for PS I isolated from either *Synechocystis* PCC6803 or *S. elongatus* and is independent of the glycerol

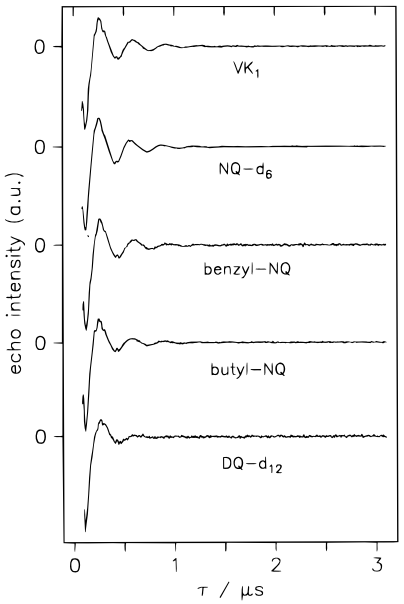

FIGURE 3: Out-of-phase echo modulations of $P_{700}^{\bullet+}A_1^{\bullet-}$ in native PS I from *Synechocystis* PCC6803 and of $P_{700}^{\bullet+}Q^{\bullet-}$ in quinone-reconstituted preparations measured at X-band and 150 K. The first 88 ns of the echo modulation is obscured by the dead time of the spectrometer. All traces have been scaled to the same intensity. The pulse lengths and other experimental parameters are given in Materials and Methods.

content of the sample. Therefore, one can conclude directly that the dipolar coupling and, thus, the $P_{700}^{\bullet+}A_1^{\bullet-}$ cofactor distance is identical in PS I isolated from either *Synechocystis* PCC6803 or *S. elongatus*. Comparison of the echo modulations for the native sample with those for the quinone-substituted PS I preparations, which are also shown in Figure 3, immediately shows that almost the same modulation frequency is present in all samples investigated here. Thus, we can conclude qualitatively that all quinone-substituted preparations have $P_{700}^{\bullet+}Q^{\bullet-}$ distances very similar to the native sample.

Besides the similarity of the modulation frequency, differences in the decay of the echo modulations are visible. The strongest damping of the echo signal is apparent in the PS I sample containing DQ-d_{12}. Different damping of the ESEEM signal has been observed previously as a function of temperature in Zn-bRCs (Dzuba *et al.*, 1995, 1997a) and in PS I as a function of the glycerol content of the sample (Zech *et al.*, 1996; Bittl & Zech, 1997). Possible explanations of the damping of the ESEEM signal are a distribution of $P_{700}^{\bullet+}Q^{\bullet-}$ distances or the mobility of the quinone in the A_1 binding pocket which determine the echo decay at low temperatures. In particular, a distribution of cofactor distances leads to a distribution of dipolar couplings and thus to a superposition of modulation frequencies. Such a superposition would then result in an echo decay faster than that for one fixed distance.

At higher temperatures, a slower decay is observed and can be explained as a result of a motional averaging of the inhomogeneous distribution of dipolar couplings. Using this interpretation of the observed ESEEM damping in native samples, the fast decay in the case of DQ-d_{12}-substituted PS I suggests a wider distribution of cofactor distances and/or a smaller mobility for this quinone. A wider distribution of $P_{700}^{\bullet+}Q^{\bullet-}$ distances for DQ-d_{12} implies that it does not bind

as specifically as the other quinones which is consistent with the observation that benzoquinones bind poorly to the A_1 site (Iwaki *et al.*, 1996). In principle, a quantitative analysis of the echo decay would yield information about the motion of the quinone (Rohrer *et al.*, 1996). However, in X-band experiments, this is not feasible in practice because no orientation selection is possible in contrast to W-band experiments.

Numerical Simulations. In our previous studies, the dipolar and isotropic couplings have been determined by a comparison of the Fourier-transformed echo modulations and numerical simulations according to the CCRP model (Zech *et al.*, 1996; Bittl & Zech, 1997). For this purpose, it is necessary to reconstruct the signal during the spectrometer dead time. Here, we will take a different approach and will compare the experimental echo modulation directly with numerical simulations in the time domain. This approach has an advantage because no signal reconstruction is necessary. The simulation according to the CCRP model requires several parameters, i.e. the **g**-tensors of $P_{700}^{\bullet+}$ and $A_1^{\bullet-}$ and the orientation of both cofactor radicals with respect to Z_D as well as the dipolar coupling D and the isotropic coupling J (Salikhov *et al.*, 1992). The dominant term responsible for the modulation of the out-of-phase echo is given by $\Gamma = 2J - 2D(\cos^2\theta - 1/3)$, where θ is the angle between the dipolar axis Z_D and the magnetic field B_0. This term depends only on the coupling between the two electron spins and is independent of any hyperfine coupling or differences in the g-factors of the electrons (Salikhov *et al.*, 1992). Therefore, the **g**-tensors and orientational parameters have a negligible influence on the simulated echo modulation, and a calculation of the cofactor distance via the dipolar coupling D is possible without knowledge of the exact orientation of each substituted quinone or its **g**-anisotropy (Bittl & Zech, 1997). Nevertheless, we have used as many parameters as possible from independent transient EPR experiments (van der Est *et al.*, 1995) for the simulation of the ESEEM traces.

It is important to note that the modulation frequency of the out-of-phase echo is not influenced by the population differences within the energy sublevels of the two-spin system. In recent studies (Dzuba *et al.*, 1996b, 1997b), it has been shown that the modulation frequency does not change, even if a part of the population is transferred within the energy levels, e.g. by a mw pulse. As a consequence, the modulation frequency should be unaffected by the lifetime of the primary RP $P_{700}^{\bullet+}A_0^{\bullet-}$ which causes a change of the relative populations of energy levels for $P_{700}^{\bullet+}Q^{\bullet-}$. This is an additional difference with respect to the transient EPR spectra of $P_{700}^{\bullet+}Q^{\bullet-}$, where the singlet−triplet mixing within a long-lived primary RP has to be taken into account especially at higher mw frequencies (Tang *et al.*, 1996).

The observed damping of the ESEEM causes a broadening of the frequency spectrum obtained by a sine Fourier transform (SFT) of the ESEEM. In the simulation shown here, this damping is taken into account phenomenologically by an exponential decay of the calculated time traces with a decay constant τ_d. The value for τ_d has been derived by a comparison between the damping of the experimental ESEEM and the calculated time signal. After τ_d was adjusted to the observed echo decay, the values for D and J were adjusted to reproduce the modulation frequency of the experimental ESEEM. As an example, the resulting simulations of the ESEEM are shown in Figure 4 for the native system and the NQ-d_6-reconstituted sample. As can be seen, the modulation frequency and the decay of the echo signal can be simulated satisfactorily. For the first 88 ns of the ESEEM, the numerical simulation does not agree well with the signal reconstruction method described previously (Zech *et al.*, 1996; Bittl & Zech, 1997). This difference is responsible for the poor coincidence between the SFT of the experimental ESEEM and its numerical simulation in the frequency range from 4 to 6 MHz shown previously (Zech *et al.*, 1996; Bittl & Zech, 1997). However, the values for D and J do not depend significantly on this part of the data.

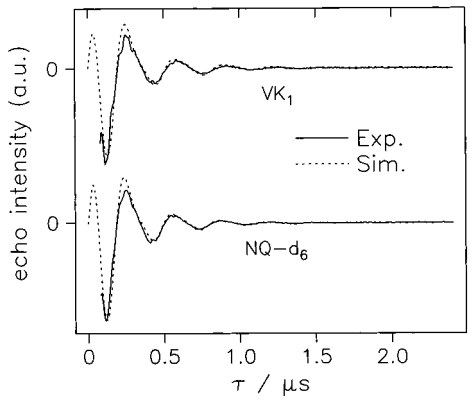

FIGURE 4: Experimental out-of-phase echo modulation of native PS I and NQ-d_6-replaced PS I (solid lines) and numerical simulations (dotted lines) according to the model of correlated coupled radical pairs. For the simulation, the **g**-tensor and cofactor orientation as obtained in transient EPR studies were used. The parameters for the dipolar coupling D obtained from these simulations are given in Table 1.

Table 1: Parameters Obtained from the Simulation of the Out-of-Phase Echo Modulation and Corresponding Cofactor Distances

quinone acceptor	dipolar coupling D (μT)	decay constant τ_d[a] (μs)	cofactor distance r (Å)
VK_1	-170 ± 4	0.40 ± 0.05	25.4 ± 0.3
NQ-d_6	-176 ± 4	0.35 ± 0.05	25.1 ± 0.3
benzyl-NQ	-167 ± 4	0.32 ± 0.04	25.6 ± 0.3
butyl-NQ	-173 ± 4	0.26 ± 0.03	25.3 ± 0.3
DQ-d_{12}	-164 ± 4	0.19 ± 0.03	25.7 ± 0.3

[a] The value for the Lorentzian line width $\Delta\nu_L$ used in a previous study (Bittl & Zech, 1997) can be calculated using $\Delta\nu_L = 1/(2\pi\tau_d)$.

The values of D and τ_d obtained from the simulation are given in Table 1. The distances between the centers of the spin densities are also given and have been derived using a point dipole model which yields the relation $r = (-2786mT/D)^{1/3}$ Å. As can be seen, the dipolar couplings and distances are almost the same for all samples within experimental error which favors the native A_1 site as the binding position for all the quinones. The same result was obtained recently for spinach PS I particles reconstituted with 2,3-dibromo-1,4-naphthoquinone (Dzuba *et al.*, 1997b).

We also obtained a J value of 1.0 ± 0.8 μT for all samples which is consistent with the simulation of the transient EPR spectra of $P_{865}^{\bullet+}Q_A^{\bullet-}$ in Zn-substituted bRCs for which only small values for J are in agreement with the experimental data (van den Brink *et al.*, 1994).

DISCUSSION

As mentioned in the introductory section, the spin-polarized EPR spectra of native PS I and NQ-d_6-substituted

PS I (van der Est *et al.*, 1995) indicate that the two quinones, VK_1 and NQ-d_6, are oriented differently. On the other hand, the out-of-phase echo modulations presented here show that this change in orientation occurs without an accompanying change in the distance between $P_{700}^{\bullet+}$ and $Q^{\bullet-}$. Thus, we can conclude that NQ-d_6 is indeed bound to the A_1 binding site but with a different orientation which means that NQ-d_6 is not hydrogen bonded to the protein in the same way as VK_1.

From the transient EPR spectra, a rotation of the *x*-axis of **g**($NQ^{\bullet-}$), i.e. the axis joining the two oxygens of the quinone, with respect to Z_D of about 90° was estimated. From this point of view, two distinct orientations of the NQ-d_6 in the A_1 binding pocket are possible. The first leads to an orientation in which the aromatic ring with the two carbonyl oxygens of the NQ-d_6 molecule is directed toward P_{700}; the second possibility yields an orientation directing the ring away from P_{700}. These two possibilities are depicted in panels B and C of Figure 5, respectively. In the figure, the quinone has been rotated around its center of spin density to keep the $P_{700}^{\bullet+}Q^{\bullet-}$ distance constant. To a good approximation, this center of spin density can be assumed to be the midpoint between the two carbonyl oxygen atoms of the quinone even if the spin density shows a slightly asymmetric distribution between these two oxygen atoms (Bittl & Zech, 1997). The slightly reduced $P_{700}^{\bullet+}Q^{\bullet-}$ distance for NQ-d_6 is not sufficient to favor the orientation shown in panel B over the orientation shown in panel C of Figure 5. However, it is evident from Figure 5 that neither orientation of NQ compared to VK_1 inside the A_1 binding pocket requires a major change of the distance between the primary donor and the quinone acceptor, although the center of spin density is located roughly in the middle of only one of the aromatic rings rather than between these two rings.

As pointed out above, the change in the orientation of the carbonyl oxygen atoms of NQ-d_6 implies that NQ-d_6 and VK_1 must be hydrogen bonded very differently. Because hydrogen bonding tends to reduce the **g**-anisotropy, the larger anisotropy for NQ-d_6, obtained from the transient K-band spectrum (van der Est *et al.*, 1995), suggests that it may not be hydrogen bonded at all. On the other hand both, ENDOR experiments on photoaccumulated $A_1^{\bullet-}$ (Heathcote *et al.*, 1995; Rigby *et al.*, 1996) and the behavior of the **g**-tensor point toward hydrogen bonding for the native VK_1. This leads to the conclusion that the function of the quinone in the A_1 binding site as an electron acceptor does not depend on its orientation or whether it is hydrogen bonded. Moreover, as shown recently (Iwaki *et al.*, 1996), quinones with a wide range of redox potentials also function as acceptors, albeit with different ET rates. The ET to F_X, on the other hand, is very sensitive to the nature of the quinone and does not occur when NQ-d_6 is substituted into PS I (Sieckmann *et al.*, 1991). This is probably mainly determined by the redox potentials of A_1 which could be influenced by the orientation, e.g. due to the presence or absence of H bonds. The observed change in the orientation between VK_1 and NQ-d_6 shown in Figure 5 would be possible if the quinone is held in place by π-type interactions with neighboring aromatic amino acid residues.

CONCLUSIONS

The determination of very similar distances between $P_{700}^{\bullet+}$ and $Q^{\bullet-}$ in all quinone exchanged preparations reported here leads to the conclusion that the artificial quinones are all bound to the A_1 site in the protein. This removes the ambiguity concerning the binding position of the reconstituted quinones which was left open by transient EPR experiments. Quinone reconstitution into sites other than the A_1 binding pocket cannot be excluded. However, such quinones, if present, do not make a significant contribution to the observed spin-polarized $P_{700}^{\bullet+}Q^{\bullet-}$ signal, since this would lead to very different echo modulations. In conclusion, the same center to center (dipolar) distance provides convincing evidence that within experimental accuracy the observed $P_{700}^{\bullet+}Q^{\bullet-}$ signals result only from the quinones substituted in the same site as A_1 in native PS I.

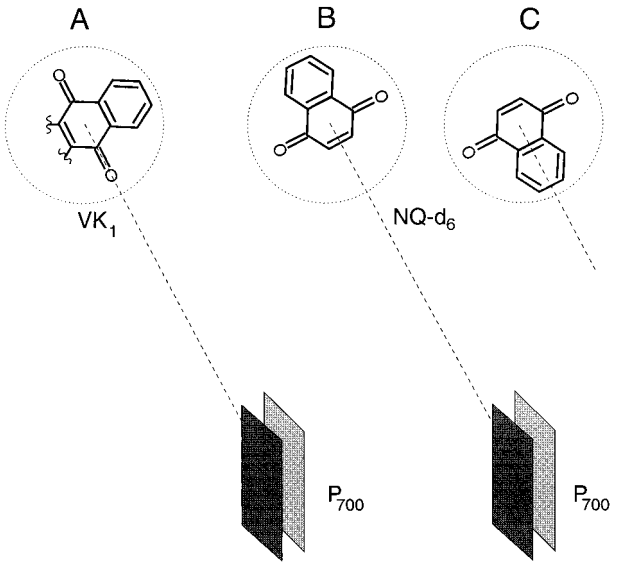

FIGURE 5: Possible orientations for native VK_1 and reconstituted NQ-d_6 in the A_1 binding pocket. (A) The carbonyl oxygens of the native VK_1 are located parallel to the dipolar axis Z_D (indicated as a dashed line). The two chlorophyll molecules forming P_{700} are indicated as rectangles. (B) The NQ-d_6 is located at the same distance from P_{700} in the A_1 binding pocket but is rotated by about 90° around the center of the spin density. The aromatic ring with the two carbonyl oxygens of the NQ-d_6 molecule is directed toward P_{700}. (C) The carbonyl oxygen ring is directed away from P_{700}. A change of the orientation of the quinone inside the A_1 binding pocket is possible without an accompanying change of the $P_{700}^{\bullet+}Q^{\bullet-}$ distance.

This observation increases the relevance of the observed differences in the spin-polarized EPR spectrum (van der Est *et al.*, 1995) with respect to the binding of the native quinone. The altered orientation for NQ-d_6 and the increase of its **g**-tensor anisotropy indicate a strong difference in the hydrogen bonding to the protein in the A_1 binding pocket for this quinone compared to the native VK_1.

ACKNOWLEDGMENT

We thank H. Zimmermann (MPI Heidelberg) and W. Oettmeier (Ruhr Universität Bochum) for providing some of the quinones and I. Sieckmann, C. Klett (Freie Universität Berlin), and H. Bottin (ECA Saclay) for preparation of the quinone-substituted PS I samples. We are grateful to W. Lubitz (Technische Universität Berlin) and to D. Stehlik (FU Berlin) for their support and helpful discussions and suggestions.

REFERENCES

Allen, J. P., Feher, G., Yeates, T. O., Komiya, H., & Rees, D. C. (1987) *Proc. Natl. Acad. Sci. U.S.A. 84*, 5730−5734.

Angerhofer, A., & Bittl, R. (1996) *Photochem. Photobiol. 63*, 11−38.
Arnoux, B., Gaucher, J.-F., Ducruix, A., & Reiss-Husson, F. (1995) *Acta Crystallogr. D 51*, 368−379.
Biggins, J., & Mathis, P. (1988) *Biochemistry 27*, 1494−1500.
Bittl, R., & Zech, S. G. (1997) *J. Phys. Chem. B 101*, 1429−1436.
Brettel, K. (1997) *Biochim. Biophys. Acta 1318*, 322−373.
Chang, C.-H., El-Kabbani, O., Tiede, D., Norris, J., & Schiffer, M. (1991) *Biochemistry 30*, 5352−5360.
Deisenhofer, J., Epp, O., Miki, K., Huber, R., & Michel, H. (1985) *Nature 318*, 618−624.
Dzuba, S. A., Gast, P., & Hoff, A. J. (1995) *Chem. Phys. Lett. 236*, 595−602.
Dzuba, S. A., Bosch, M. K., & Hoff, A. J. (1996a) *Chem. Phys. Lett. 248*, 427−433.
Dzuba, S. A., Proskuryakov, I. I., Hulsebosch, R. J., Bosch, M. K., Gast, P., & Hoff, A. J. (1996b) *Chem. Phys. Lett. 253*, 361−366.
Dzuba, S. A., Gast, P., & Hoff, A. J. (1997a) *Chem. Phys. Lett. 268*, 273−279.
Dzuba, S. A., Hara, H., Kawamori, A., Iwaki, M., Itoh, S., & Tsvetkov, Y. D. (1997b) *Chem. Phys. Lett. 264*, 238−244.
Ermler, U., Fritzsch, G., Buchanan, S. K., & Michel, H. (1994) *Structure 2*, 925−936.
Heathcote, P., Rigby, S., & Evans, M. (1995) in *Photosynthesis: from Light to Biosphere* (Mathis, P., Ed.) Vol. II, pp 163−166, Kluwer Academic Publishers, Dordrecht, The Netherlands.
Iwaki, M., Kumazaki, S., Yoshita, K., Erabi, T., & Itoh, S. (1996) *J. Phys. Chem. 100*, 10802−10809.
Krauss, N., Schubert, W.-D., Klukas, O., Fromme, P., Witt, H. T., & Saenger, W. (1996) *Nat. Struct. Biol. 3*, 965−973.
Lüneberg, J., Fromme, P., Jekow, P., & Schlodder, E. (1994) *FEBS Lett. 338*, 197−202.
Moënne-Loccoz, P., Heathcote, P., Maclachlan, D. J., Berry, M. C., Davis, I. H., & Evans, M. C. W. (1994) *Biochemistry 33*, 10037−10042.
Rigby, S. E. J., Evans, M. C. W., & Heathcote, P. (1996) *Biochemistry 35*, 6651−6656.
Rohrer, M., Gast, P., Möbius, K., & Prisner, T. (1996) *Chem. Phys. Lett. 259*, 523−530.
Salikhov, K. M., Kandrashkin, Y. E., & Salikhov, A. K. (1992) *Appl. Magn. Reson. 3*, 199−216.
Schlodder, E., Brettel, K., Falkenberg, K., & Gergeleit, M. (1995) in *Photosynthesis: from Light to Biosphere* (Mathis, P., Ed.) Vol. II, pp 107−110, Kluwer Academic Publishers, Dordrecht, The Netherlands.
Sieckmann, I., van der Est, A., Bottin, H., Sétif, P., & Stehlik, D. (1991) *FEBS Lett. 284*, 98−102.
Stehlik, D., Bock, C. H., & Petersen, J. (1989) *J. Phys. Chem. 93*, 1612−1619.
Tang, J., Thurnauer, M. C., & Norris, J. R. (1994) *Chem. Phys. Lett. 219*, 283−290.
Tang, J., Bondeson, S., & Thurnauer, M. C. (1996) *Chem. Phys. Lett. 253*, 293−298.
van den Brink, J. S., Hulsebosch, R. J., Gast, P., Hore, P. J., & Hoff, A. J. (1994) *Biochemistry 33*, 13668−13677.
van der Est, A., Bock, C., Golbeck, J., Brettel, K., Sétif, P., & Stehlik, D. (1994) *Biochemistry 33*, 11789−11797.
van der Est, A., Sieckmann, I., Lubitz, W., & Stehlik, D. (1995) *Chem. Phys. 194*, 349−359.
van der Est, A., Prisner, T., Bittl, R., Fromme, P., Lubitz, W., Möbius, K., & Stehlik, D. (1997) *J. Phys. Chem. B 101*, 1437−1443.
Witt, H. T. (1996) *Ber. Bunsen-Ges. Phys. Chem. 100*, 1923−1942.
Zech, S. G., Lubitz, W., & Bittl, R. (1996) *Ber. Bunsen-Ges. Phys. Chem. 100*, 2041−2044.

BI970754Z